Reduction of sound-evoked midbrain responses observed by functional magnetic resonance imaging following acute acoustic noise exposure

Bin Yang, Eddie Wong, Wai Hong Ho, Condon Lau, Ying Shing Chan, and Ed X. Wu

Citation: The Journal of the Acoustical Society of America **143**, 2184 (2018); doi: 10.1121/1.5030920
View online: https://doi.org/10.1121/1.5030920
View Table of Contents: https://asa.scitation.org/toc/jas/143/4
Published by the Acoustical Society of America

Reduction of sound-evoked midbrain responses observed by functional magnetic resonance imaging following acute acoustic noise exposure

Bin Yang, Eddie Wong, Wai Hong Ho, and Condon Lau[a)]
Department of Physics, The City University of Hong Kong, Hong Kong, People's Republic of China

Ying Shing Chan
School of Biomedical Sciences, The University of Hong Kong, Hong Kong, People's Republic of China

Ed X. Wu
Department of Electrical and Electronic Engineering, The University of Hong Kong, Hong Kong, People's Republic of China

(Received 2 August 2017; revised 18 March 2018; accepted 23 March 2018; published online 19 April 2018)

Short duration and high intensity acoustic exposures can lead to temporary hearing loss and auditory nerve degeneration. This study investigates central auditory system function following such acute exposures after hearing loss recedes. Adult rats were exposed to 100 dB sound pressure level noise for 15 min. Auditory brainstem responses (ABRs) were recorded with click sounds to check hearing thresholds. Functional magnetic resonance imaging (fMRI) was performed with tonal stimulation at 12 and 20 kHz to investigate central auditory changes. Measurements were performed before exposure (0D), 7 days after (7D), and 14 days after (14D). ABRs show an ~6 dB threshold shift shortly after exposure, but no significant threshold differences between 0D, 7D, and 14D. fMRI responses are observed in the lateral lemniscus (LL) and inferior colliculus (IC) of the midbrain. In the IC, responses to 12 kHz are $3.1 \pm 0.3\%$ (0D), $1.9 \pm 0.3\%$ (7D), and $2.9 \pm 0.3\%$ (14D) above the baseline magnetic resonance imaging signal. Responses to 20 kHz are $2.0 \pm 0.2\%$ (0D), $1.4 \pm 0.2\%$ (7D), and $2.1 \pm 0.2\%$ (14D). For both tones, responses at 7D are less than those at 0D ($p < 0.01$) and 14D ($p < 0.05$). In the LL, similar trends are observed. Acute exposure leads to functional changes in the auditory midbrain with timescale of weeks.
 https://doi.org/10.1121/1.5030920

[GCS] Pages: 2184–2194

I. INTRODUCTION

Effective hearing is one of the key factors for humans and animals to survive and prosper in an increasingly competitive world. The auditory system enables us to detect and process sounds, including sounds with fine temporal and spectral differences. This facilitates verbal communication and, for non-human animals, distinguishing predators from prey. The auditory system can be damaged by high sound pressure level (SPL) exposures, which are present in many developed and developing regions. Possibly the most recognized form of damage is noise-induced hearing loss (NIHL), which is a major health issue (NIDCD, 2014). NIHL involves a permanent elevation of hearing thresholds, resulting in reduced hearing sensitivity. Permanent threshold shifts are typically due to prolonged exposures to high SPL sounds. To protect against permanent hearing loss, the National Institute for Occupational Safety and Health recommends against noise exposures exceeding 85 dBA for 8 h/day (NIOSH, 1998).

Prolonged and acute acoustic exposures (short duration and high SPL) may also lead to a temporary threshold shift that disappears 16–48 h later (NIDCD, 2014). Recent research suggests that temporary hearing loss may be more harmful than previously thought (Liberman, 2015). In a landmark series of studies, Kujawa, Liberman, and colleagues exposed mice (and other rodents) to 100 dB SPL noise for 2 h (Kujawa and Liberman, 2009; Lin *et al.*, 2011). This exposure induced a temporary hearing loss with timescale of weeks. However, significant loss of auditory nerve synapses was seen after one day. The rest of the auditory nerve, including the cell body and axons projecting to the brain, degenerated over the coming months. This degeneration showed no signs of recovery. This permanent damage (hidden hearing loss) does not significantly affect the ability to detect sounds, but may hamper the ability to process more complicated acoustic signals (Liberman, 2015). This, in turn, can affect the ability to process the subtle signals in speech.

The above understanding of the impact of acute acoustic exposures is primarily of the auditory periphery. Considering that sound detection is largely unaffected, we investigate the impact of acute exposure on the central auditory system. In particular, we focus on the time period after the temporary threshold shift recedes. The central auditory studies will be performed primarily with functional magnetic resonance imaging (fMRI). fMRI is a non-invasive technique with large field of view (FOV) that is able to simultaneously investigate multiple brain structures with relatively high spatial

[a)]Electronic mail: condon.lau@cityu.edu.hk

resolution. fMRI is well suited to longitudinal studies. Further, fMRI can complement electrophysiological and immunohistochemistry studies by directing the investigation sites and facilitating the translation of results to humans, where fMRI is regularly performed. Blood oxygenation level dependent (BOLD) contrast fMRI (Ogawa *et al.*, 1990) has been widely adopted for different types of sensory and cognitive investigations. For the auditory system, BOLD fMRI studies have been conducted to investigate auditory information processing (Friederici *et al.*, 2000; Maeder *et al.*, 2001; Koelsch *et al.*, 2005; Holland *et al.*, 2008; Wu and Lin, 2008). A number of studies have applied BOLD fMRI in humans to investigate the underlying mechanism of hearing loss and hearing disorders such as tinnitus (Bilecen *et al.*, 2000; Jancke *et al.*, 2001; Schmithorst *et al.*, 2005; Smits *et al.*, 2007; Lanting *et al.*, 2008; Gu *et al.*, 2010). Relatively fewer animal auditory fMRI studies have been reported so far (Van Meir *et al.*, 2005; Boumans *et al.*, 2007; Kayser *et al.*, 2007; Voss *et al.*, 2007; Tanji *et al.*, 2010; Baumann *et al.*, 2011; Bach *et al.*, 2013; Brown *et al.*, 2013; Butler *et al.*, 2015; Hall *et al.*, 2016; Ortiz-Rios *et al.*, 2017). The results from these studies demonstrate that auditory fMRI studies on animals can provide valuable insights into hearing mechanisms, especially in subcortical structures such as the inferior colliculus (IC). Our group has developed functional and structural magnetic resonance imaging (MRI) methods for auditory investigations in the experimentally versatile rat model (Cheung *et al.*, 2012a; Cheung *et al.*, 2012b; Lau *et al.*, 2013; Zhang *et al.*, 2013; Gao *et al.*, 2014; Gao *et al.*, 2015a; Lau *et al.*, 2015a; Lau *et al.*, 2015b; Abdoli *et al.*, 2016; Wong *et al.*, 2017).

In this study, adult rat subjects were exposed to broadband acoustic noise at 100 dB SPL for 15 min. Auditory fMRI was performed on each subject at three time points: immediately before the acute exposure (0D), 7 days after the exposure (7D), and 14 days after (14D). Auditory brainstem responses (ABRs) were also acquired at the three time points, plus an additional time point shortly after the exposure (0D+), to check for significant hearing threshold shifts. This will allow fMRI findings from the central auditory system to be interpreted without the confound of a significant threshold shift. The results of this study are important for understanding the impact of acute noise exposures on central auditory function.

II. METHODS

A. Animal subjects

All animal experiments were approved by the animal research ethics committees of the City University of Hong Kong, the University of Hong Kong, and the Department of Health of the Hong Kong Special Administrative Region. Adult female Sprague-Dawley rats (250–260 g, N = 14) were employed in this study. Females were chosen to minimize size change during the course of the 14 days study. Figure 1 illustrates the study design. Upon entering the study, subjects first underwent brain imaging or ABR testing, followed by acute noise exposure, before being placed in housing. Imaging was performed before the exposure (0D), 7 days after (7D), and 14 days after (14D). Subjects were housed in pairs in standard cages throughout the study. Food and water were provided *ad libitum* and the holding room had a 12 h light/dark cycle. The background SPL in a cage was <40 dB.

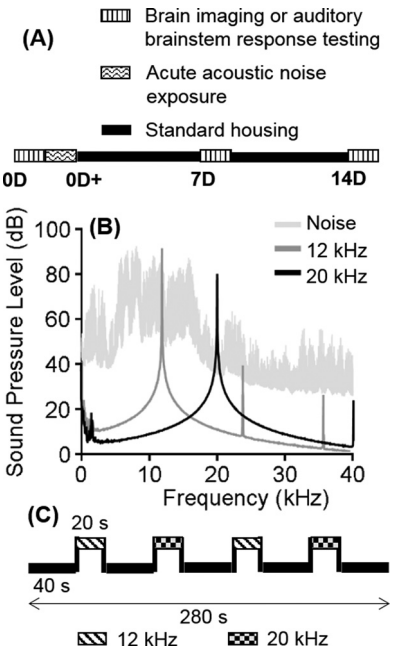

FIG. 1. (A) Study design showing the three time points where fMRI and ABR recording are performed. The first time point (day 0, 0D) occurs just before the 15 min, 100 dB SPL acute acoustic noise exposure. Time points 7D and 14D are 7 and 14 days after the exposure, respectively. In between time points, the subjects are in standard housing. ABRs are recorded at an additional time point (0D+) shortly after the noise exposure. (B) Acoustic power spectra of the noise exposure and acoustic stimuli. The exposure is a 100 dB total SPL broadband noise peaked between 8 and 16 kHz. The two stimuli are 12 and 20 kHz tones at 90 and 80 dB SPL, respectively. (C) Representative fMRI block-design stimulation paradigm with four 20 s ON periods interleaved between 40 s OFF periods. During ONs, one of the tones is played. During OFFs, there is no stimulation. The order of tone presentation is pseudorandom (see Sec. II, Methods). MRI image acquisition occurs every 1 s throughout the 280 s paradigm.

B. Acute acoustic noise exposure

The acute exposure was a broadband acoustic noise, peaked between 8 and 16 kHz, at 100 dB total SPL (SPL_t) presented binaurally for 15 continuous minutes. The bandwidth and SPL of the exposure were measured and calibrated with a 50 kHz microphone (M50, Earthworks Audio, Milford, NH) and a 192 kHz recorder (FR2, Fostex, Norwalk, CA). $SPL_t = 10 \log \left(\sum_{k=1}^{n} 10^{SPL(k)/10}\right)$, where $k = 1$–n are the sampling frequencies of the microphone. Figure 1 shows the acoustic power spectrum of the noise. During exposure, subjects were placed individually within a cage and the cage was placed inside of an enclosed chamber. A loudspeaker (H-600Q, T&T, Shenzhen, China) was placed 15 cm above the center of the cage. Microphone measurements were performed before each exposure session with the microphone placed in the center of the cage at the height of the subject's ears.

C. ABR

ABRs were recorded at 0D, shortly after noise exposure (0D+), 7D, and 14D ($N = 4$). Note that 0D and 0D+

recordings were made from two subjects and 0D, 7D, and 14D recordings were made from two separate subjects. Subjects were anesthetized by intraperitoneal injection of sodium pentobarbital (50 mg/kg). Recordings were performed inside a sound attenuating chamber (IAC Acoustics, Winchester, UK). Body temperature was maintained by placing the subject in contact with a heat pad. Three subdermal needle electrodes were inserted about the ear for recording the ABR. The positive electrode was inserted at the vertex, the negative electrode below the pinna of the left ear facing the speaker (ALT-800, ProAudio, Hong Kong, China), and the ground electrode at the back of the subject. Note that for the two subjects with recordings at 0D+, anesthetic was administered and the electrodes inserted prior to noise exposure such that recordings began less than 10 min after the exposure. Click sounds of 0.1 ms duration were used to stimulate the ear every 100 ms. The SPL at the position of the ear canal was measured and calibrated with the 50 kHz microphone and 192 kHz recorder. The SPL was decreased in at least 6 dB steps by lowering speaker output. Below 25 dB, SPL was decreased by increasing the distance between the speaker and the subject as this method led to more consistent microphone measurements. Each subject was stimulated with 1024 clicks at each SPL and the average response at each SPL was recorded. The threshold was defined as the lowest SPL setting with a consistent, clearly discernible response. The amplitudes of waves I and IV at 50 dB SPL was defined as the peak-to-peak amplitude.

D. Subject preparation for imaging

Subjects were prepared for imaging sessions at each time point (0D, 7D, and 14D) in a similar manner to our previous studies (Lau *et al.*, 2013; Gao *et al.*, 2014; Gao *et al.*, 2015a; Gao *et al.*, 2015b; Lau *et al.*, 2015a; Lau *et al.*, 2015b; Wong *et al.*, 2017). Subjects ($N = 10$) were anesthetized with 1% isoflurane (3% to induce anesthesia) and mechanically ventilated (TOPO, Kent Scientific, Torrington, CT) via oral intubation. They were then placed on a body holder in the prone position with a tooth bar and nose cone to restrict head motion. A custom 165 cm long rigid sound tube with a 6.5 cm flexible distal end was placed in the left ear canal of the subject. The right ear was occluded with cotton wool and Vaseline (Unilever, Rotterdam, Netherlands). A pulse oximeter was connected to a hind paw to monitor heart rate and saturation of peripheral oxygen. A rectum thermometer was used to monitor body temperature, which was maintained by circulating warm water through the holder. A pressure sensor was positioned on the subject to monitor respiration rate. A capnograph was connected to the exhaust port of the ventilator to monitor end-tidal CO_2. All vital signs sensors were from SA Instruments (Stony Brook, NY). The MRI surface coil was placed over the head, centered between the ears and above the midbrain, and the entire setup was placed inside of the scanner.

E. Acoustic stimulation

Acoustic stimulation during fMRI was produced by a broadband magnetic speaker (MF1, Tucker-Davis Technologies, Alachua, FL) driven by a matching amplifier (SA1, Tucker-Davis Technologies). The speaker was placed at the proximal end of the sound tube to deliver monaural stimulation. Two tonal stimuli of 12 and 20 kHz were employed in this study. Figure 1 shows the acoustic power spectra of the tones. The SPLs of the tones were approximately 90 and 80 dB, respectively. These SPLs corresponded to the maximum output of the speaker at the respective frequencies. SPL measurements were performed by placing the 50 kHz microphone at the distal end of the tube, which enters the ear canal. Note that the low frequency tone was at higher SPL as the speaker's output had to propagate down the long sound tube. The tones were presented in a block design paradigm temporally synchronized with image acquisition. The paradigm consisted of an initial 40 s without stimulation (OFF) followed by four blocks of 20 s with stimulation (ON) and 40 s OFF. The total paradigm duration was 280 s. During each ON period, the 12 or 20 kHz tone was presented to the subject. The paradigm is illustrated in Fig. 1. The tones were amplitude modulated with 100% modulation depth and 50% duty cycle. The paradigm was presented ten times to each subject at each time point with one minute rest intervals. The tones were presented in pseudorandom order, with the constraint that each frequency was presented in an equal number of ON periods after the ten paradigm presentations.

F. Image acquisition

Imaging was performed by placing the subject inside of a 7 T MRI scanner (PharmaScan, Bruker Biospin, Billerica, MA) using a transmit-only birdcage coil in combination with an actively decoupled receive-only surface coil. Scout images were first acquired to determine the orientation of the brain relative to the scanner. A 1.2 mm coronal slice was then positioned to be centered on the IC of the midbrain according to the rat brain atlas (Paxinos and Watson, 2005). A set of four coronal slices, spaced 0.2 mm apart, was positioned with the above slice second from the posterior of the brain. The scan geometry is illustrated in Fig. 2 on a sagittal view of the brain at midline. An anatomical image was acquired for reference using the following sequence parameters: rapid acquisition with relaxation enhancement (RARE), RARE factor = 8, FOV = 32×32 mm^2, data matrix = 256×256, echo time (TE) = 32 ms, and repetition time (TR) = 4.2 s. fMRI images were acquired using the following sequence parameters: single-shot gradient-echo echo-planar imaging (GE-EPI), FOV = 32×32 mm^2, data matrix = 64×64, flip angle = 56°, TE = 20 ms, TR = 1000 ms, and repetitions = 280 (total of 280 s). Each fMRI acquisition was temporally synchronized with stimulus presentation and constituted a fMRI scan. Ten scans were performed at each time point separated by one minute.

G. Image processing

The image processing procedures were adapted from our recent rat auditory fMRI studies (Cheung *et al.*, 2012a; Cheung *et al.*, 2012b; Lau *et al.*, 2013; Zhang *et al.*, 2013; Gao *et al.*, 2014; Gao *et al.*, 2015a; Gao *et al.*, 2015b; Lau *et al.*, 2015a; Lau *et al.*, 2015b; Wong *et al.*, 2017). The

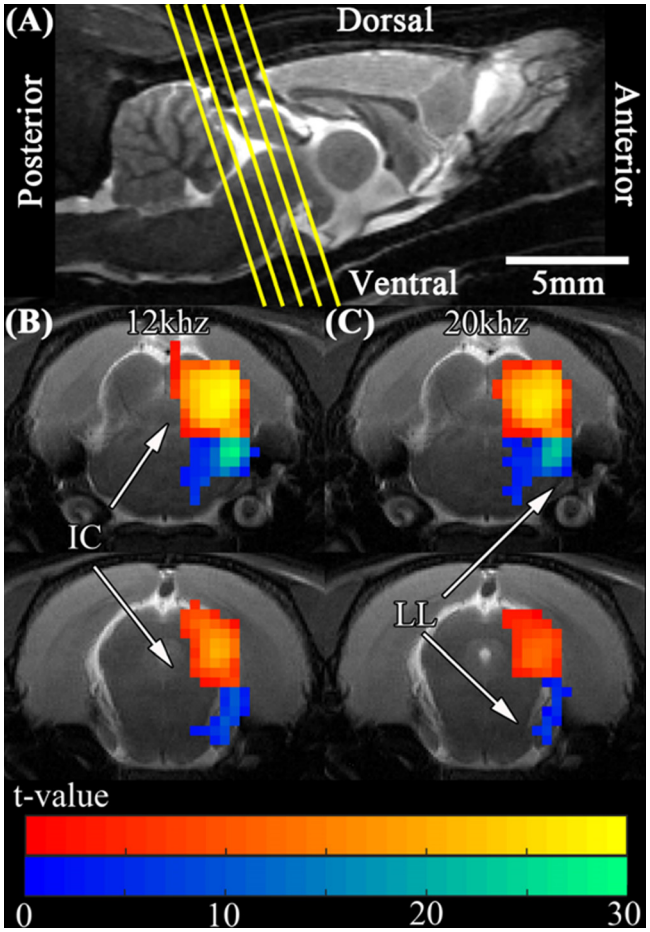

FIG. 2. (Color online) (A) fMRI scan geometry overlaid on a sagittal view of the brain at midline. The dorsal, ventral, anterior, and posterior sides of the brain are shown. (B) and (C) fMRI *t*-value maps averaged across all subjects ($N = 10$) and time points. Average activation maps acquired with 12 (B) and 20 kHz (C) acoustic stimulation are overlaid on an anatomical image. The top image slice is centered on the IC and the lower slice is 1.4 mm anterior. Monaural acoustic stimulation primarily activates the LL and IC, in the hemisphere contralateral to the simulated ear (left), of the midbrain. The IC response during 12 kHz stimulation is slightly dorsal of the 20 kHz response, reflecting the tonotopic organization of the IC. ROIs are defined spanning the LL and IC during 12 and 20 kHz stimulation (four ROIs in total, see Sec. II, Methods). The ROIs are color coded and used to compute the BOLD signals. The *t*-values in the LL (blue) and IC (red) are coded by the shade of each color.

images from all ten fMRI scans at each time point (0D, 7D, and 14D) were realigned to the mean image of the first scan with Statistical Parametric Mapping (SPM) (Wellcome Trust Centre, London, UK). Images from different subjects were than registered to the mean image of a subject at 0D, which served as the template. For registration, images were smoothed in-plane with a 0.5 mm Gaussian filter and only brain structures were included. The images were split into 60 images long sets (60 s) starting 5 s before a 20 s ON period and ending 35 s after the ON period. Sets with the same stimulation frequency (12 or 20 kHz) and from the same time point were averaged, resulting in one 60 images set for each subject at each frequency and time point. Functional activation (*t*-value) maps were computed from the image sets using SPM and custom MATLAB (The Mathworks, Natick, MA) scripts. Voxels with $p < 0.001$ and cluster size ≥ 3 were defined as activated voxels.

Regions of interest (ROIs) were functionally defined to quantify the amplitude of fMRI responses from activated structures in the central auditory system. For this purpose, average *t*-value maps were computed after averaging image sets from the same stimulation frequency across all subjects and time points. This resulted in two average *t*-value maps, one for each stimulation frequency (12 and 20 kHz). ROIs were defined for the contralateral (right) lateral lemniscus (LL) and IC as those were the structures with large *t*-values across all time points. Only voxels with $p < 0.001$ and within one voxel width of an auditory structure, according to the rat brain atlas (Paxinos and Watson, 2005), were included in the ROI of that structure. The one voxel margin was used to account for smoothing during image processing. This ROI definition ensured that ROIs spanned the same voxels in images acquired from different time points. Separate ROIs were defined for 12 and 20 kHz responses to account for the tonotopic organization of the auditory system.

BOLD signals were computed for each structure, subject, time point, and stimulation frequency by averaging the 60 s time courses from all voxels in the ROI. The corresponding BOLD signal amplitude was defined as [(average value of signal during the ON period)/(average value of signal during the 5 s before the ON period) − 1] × 100%. This definition presented the signal amplitudes in units of % baseline MRI signal.

Center of activation (COA) was computed for the IC at 12 and 20 kHz stimulation at each time point, and after averaging across time points. $\overline{r_{\mathrm{COA}}} = (1/\sum_{i=1}^{V} S_i)\sum_{i=1}^{V} S_i r_i$, where $\bar{r}$ is the coordinate relative to the interaural line (Paxinos and Watson, 2005), V is the number of activated voxels in the IC, and S is the BOLD signal (Lau *et al.*, 2015a).

H. Statistical analysis

One-way repeated measures analysis of variance (ANOVA) followed by Tukey's honest significant difference (HSD) test was employed to quantify differences between signal amplitudes and COAs from different time points.

III. RESULTS

A. ABRs

Figure 3 shows the near-threshold ABRs recorded from two subjects before acute acoustic noise exposure (0D) and immediately after (0D+). ABRs were recorded from suprathreshold SPLs down to near the hearing threshold. Responses are largest at SPLs well above threshold and become smaller near the threshold. SPL of 11 dB was the lowest at which consistent responses were observed at any time point using our ABR system. This is the threshold for all subjects at 0D. At 0D+, the threshold is 17 dB for all subjects, indicating a 6 dB threshold shift.

Figure 4 shows the near-threshold and suprathreshold ABRs from two subjects at 0D, 7 days after noise exposure (7D), and 14 days after (14D). The threshold for all subjects at 0D, 7D, and 14D is 11 dB SPL. Comparing across the three time points at 11 dB, there is little difference in

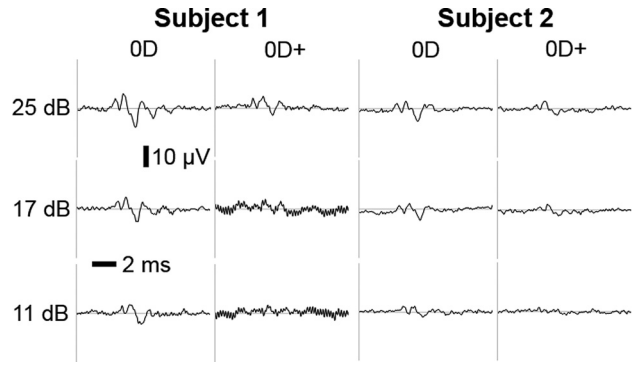

FIG. 3. ABR recordings from subjects ($N = 2$) at 0D and 0D+. ABRs are recorded with 0.1 ms click sounds from 11 dB SPL, near the hearing threshold, to suprathreshold levels. At 0D, responses are clearly discernible at all SPLs. At 0D+, responses are clearly discernible at 17 dB and above. Therefore, the acute noise exposure employed in this study causes a hearing threshold shift.

responses. The acute noise exposure employed in this study causes a short lasting temporary threshold shift and does not significantly affect the amplitude of near-threshold ABRs one and two weeks later. The suprathreshold ABRs, recorded during 50 dB SPL stimulation, show multiple waves. The amplitude of wave I at 0D is 9.2/5.4 μV (subject 1/2). For 7D and 14D, the amplitudes are 15.3/16.2 and 6.2/0.6 μV, respectively. Wave I amplitudes measured at 7D are larger than those measured at 0D. Amplitudes at 14D are smaller than those at 0D. The wave IV amplitudes at 0D, 7D, and 14D are 26.0/16.6, 30.5/17.1, and 23.8/13.7 μV, respectively. Wave IV amplitudes are largest at 7D and lowest at 14D. The ratios of wave amplitudes (I divided by IV) at 0D, 7D, and 14D are 0.35/0.33, 0.50/0.95, and 0.26/0.04, respectively.

B. Auditory midbrain responses

Figures 2(B) and 2(C) show the average t-value maps (averaged across subjects and time points) for 12 and 20 kHz stimulation, respectively. Significant responses are observed in the midbrain structures LL and IC in the hemisphere contralateral to the simulated ear. This is consistent with earlier auditory fMRI studies of the rat midbrain (Cheung *et al.*, 2012b; Lau *et al.*, 2013; Gao *et al.*, 2014; Gao *et al.*, 2015a; Gao *et al.*, 2015b; Lau *et al.*, 2015a). LL responses are largest in the dorsal nucleus while IC responses are largest in the central nucleus and external cortex. The 12 and 20 kHz ROIs were defined according to the responsive regions in these t-value maps and the rat brain atlas (Paxinos and Watson, 2005). The ROIs were used to compute the BOLD signals from different structures. Comparing the 12 and 20 kHz responses in the IC, lower sound frequencies activate more dorsal regions while higher frequencies activate more ventral regions [$F(1,78) = 4.71$, $p = 0.033$]. This is quantified by the COAs computed in Table I.

C. Reduction in fMRI signals

Figure 5 shows the fMRI t-value maps acquired at 0D, 7D, and 14D. The maps were averaged across all subjects and overlaid on an anatomical image. The largest responses in both the LL and IC are observed at 0D for both 12 and 20 kHz stimulation. At 7D, the responses are smaller in the LL and IC. At 14D, there is partial recovery in the responses toward 0D levels. Supplementary Fig. 1 shows the BOLD signals from the LL and IC at each time point and stimulation frequency.[1] The observed response reduction and recovery occur across all sound activated nuclei in the midbrain. Acute exposure leads to a reduction in auditory midbrain responses with timescale of weeks.

Table I shows the COAs in the IC during 12 and 20 kHz stimulation at 0D, 7D, and 14D. The trend of lower sound frequencies activating more dorsal regions is consistent with the time point averaged calculation. However, statistical significance is not reached for individual time points.

Figure 6 shows the t-value difference maps during 12 and 20 kHz stimulation averaged across all subjects and overlaid on an anatomical image. The difference maps were obtained by computing the difference between two of the 0D, 7D, and 14D t-value maps of Fig. 5. For the 7D–0D map, most of the auditory midbrain has negative values, indicating smaller responses one week after exposure. For the 14D–7D map, most of the auditory midbrain has positive values, indicating recovery of responses toward pre-exposure values two weeks after. Slightly negative values are observed in parts of the LL at 12 and 20 kHz stimulation, suggesting LL recovery may take a longer time or be less

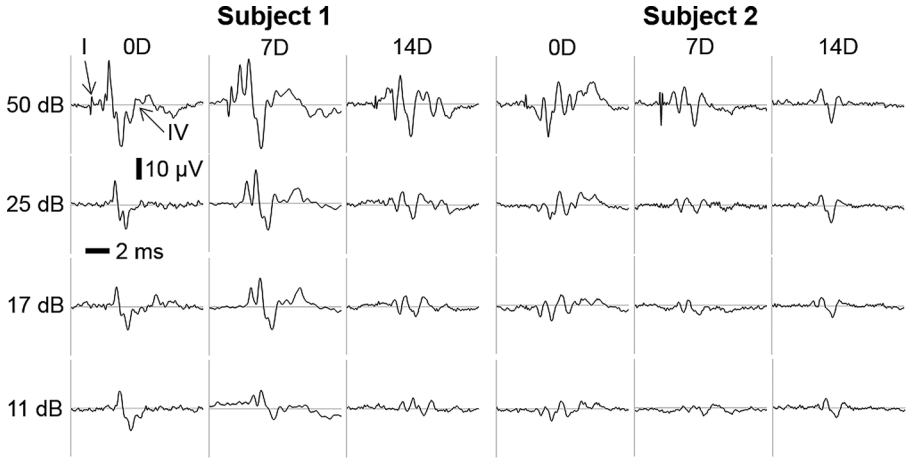

FIG. 4. ABR recordings from subjects ($N = 2$, different from the two in Fig. 3) at 0D, 7D, and 14D. ABRs recorded at 0D, 7D, and 14D near the threshold are similar, with responses clearly discernible down to 11 dB stimulation SPL. Therefore, the noise exposure causes a temporary threshold shift and thresholds recover by 7D when fMRI is performed. In the suprathreshold recording (50 dB SPL), waves I–IV (labeled I and IV) are discernible in most of the ABRs. Wave I amplitudes are largest at 7D and smallest at 14D. Similarly, wave IV amplitudes are largest at 7D and smallest at 14D, but the relative change with time is less.

TABLE I. COAs computed for the IC at 12 and 20 kHz stimulation at each time point (0D, 7D, 14D), and after averaging across time points. Mean and standard error are presented. Refer to Sec. II, Methods, for more details. The coordinates are relative to the interaural line and in units of millimeters. Statistical details, as computed by ANOVA followed by Tukey's HSD test, are given for significant differences between 12 and 20 kHz. "*" indicates $p < 0.05$ and "ns" indicates not significant.

	Time point	12 kHz	20 kHz	Significance
Dorsal of interaural line (mm)	0D	5.9 ± 0.4	5.4 ± 0.3	ns
	7D	5.8 ± 0.3	5.5 ± 0.3	ns
	14D	5.7 ± 0.4	5.3 ± 0.4	ns
	Averaged	5.8 ± 0.3	5.4 ± 0.2	*
Anterior of interaural line (mm)	0D	0.6 ± 0.2	0.6 ± 0.2	ns
	7D	0.6 ± 0.2	0.6 ± 0.1	ns
	14D	0.6 ± 0.1	0.6 ± 0.1	ns
	Averaged	0.6 ± 0.1	0.6 ± 0.1	ns
From midline (mm)	0D	2.7 ± 0.4	2.7 ± 0.4	ns
	7D	2.6 ± 0.3	2.7 ± 0.3	ns
	14D	2.8 ± 0.3	2.6 ± 0.4	ns
	Averaged	2.7 ± 0.2	2.6 ± 0.3	ns

complete than IC recovery. For the 14D–0D map, most of the auditory midbrain has negative values close to 0, indicating partial recovery of responses two weeks after exposure.

Figure 7 shows the BOLD signal amplitudes in the IC at 0D, 7D, and 14D during 12 and 20 kHz stimulation. The signals at 0D, 7D, and 14D during 12 kHz stimulation are $3.1 \pm 0.3\%$, $1.9 \pm 0.3\%$, and $2.9 \pm 0.3\%$, respectively. During 20 kHz stimulation, the signals are $2.0 \pm 0.2\%$ (0D), $1.4 \pm 0.2\%$ (7D), and $2.1 \pm 0.2\%$ (14D). The IC BOLD signal is reduced at 7D and shows signs of recovery at 14D. Using ANOVA, the signals during 12 [$F(2,27) = 7.22$, $p = 0.0031$] and 20 kHz [$F(2,27) = 5.26$, $p = 0.012$] stimulation are significantly different at the three time points. Applying Tukey's test to compare between time points, signals at 7D are significantly less than those at 0D ($p < 0.01$) and 14D ($p < 0.05$) during both stimulation frequencies. Signals at 0D and 14D are not significantly different.

Figure 8 shows the BOLD signal amplitude in the LL at 0D, 7D, and 14D during 12 and 20 kHz stimulation. The signals at 0D, 7D, and 14D during 12 kHz stimulation are $1.7 \pm 0.3\%$, $0.6 \pm 0.1\%$, and $1.4 \pm 0.3\%$, respectively. During 20 kHz stimulation, the signals are $1.1 \pm 0.2\%$ (0D), $0.5 \pm 0.1\%$ (7D), and $1.0 \pm 0.1\%$ (14D). In general, responses are largest at 0D and smallest at 7D for both frequencies. The LL BOLD signal is reduced 7 days post exposure and shows signs of recovery by 14 days, although pre-exposure values are not fully recovered. By ANOVA, there are no statistically significant differences between 0D, 7D, and 14D. However, the overall trend is similar to that in the IC. The fMRI results show that acute exposure reduces auditory midbrain responses at 7 days post exposure and partial recovery is seen at 14 days.

IV. DISCUSSION

A. Spontaneous neural activity

Acoustic trauma has been found to increase spontaneous firing rates in the IC of a range of animal species (Ma *et al.*, 2006; Mulders and Robertson, 2009; Dong *et al.*, 2010; Manzoor *et al.*, 2012; Coomber *et al.*, 2014). For example, Mulders *et al.* exposed guinea pigs to 124 dB SPL sound for 1 h (Mulders *et al.*, 2010) and observed high spontaneous activity in the IC. Such hyperactivity has been associated with tinnitus and was observed with high SPL exposures that caused significant hearing threshold shifts. The IC hyperactivity is initially dependent on input from lower auditory centers such as the cochlear nucleus and cochlea, but after weeks, may become less dependent (Mulders and Robertson, 2011; Robertson *et al.*, 2013). Similar hyperactivity has also been observed (in IC and other brain regions) following exposures that only induce temporary threshold shifts (Basura *et al.*, 2015; Hesse *et al.*, 2016; Wu *et al.*, 2016), as in this study.

BOLD fMRI signals are closely related to the local neural activity (Logothetis *et al.*, 2001; Logothetis and Wandell,

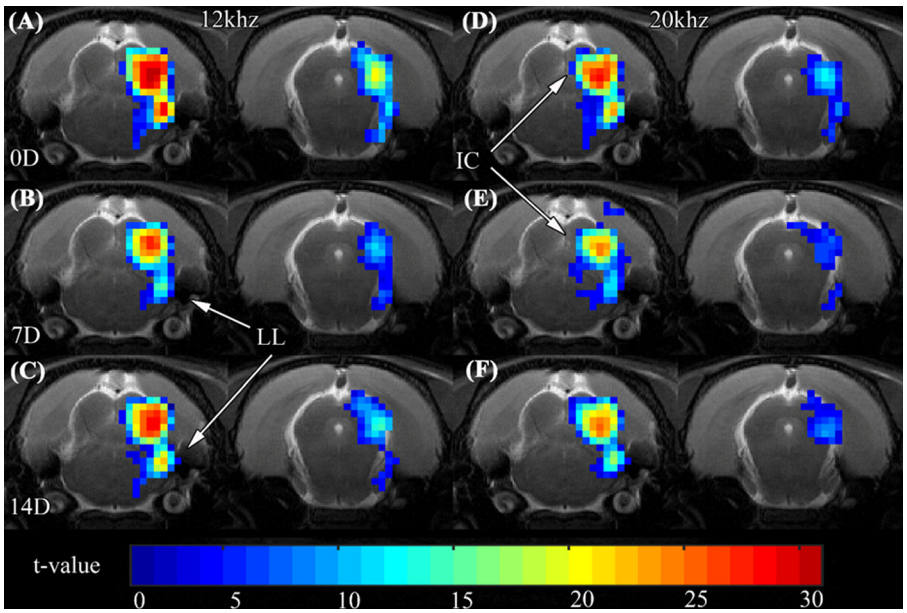

FIG. 5. (Color online) fMRI group averaged *t*-value maps at 0D, 7D, and 14D. Activation maps acquired with 12 and 20 kHz acoustic stimulation are overlaid on an anatomical image. (A) 0D, 12 kHz; (B) 7D, 12 kHz; (C) 14D, 12 kHz; (D) 0D, 20 kHz; (E) 7D, 20 kHz; (F) 14D, 20 kHz. Responses are primarily observed in the contralateral (right) LL and IC. Responses at 7D are significantly lower than those at 0D and 14D. This trend is similar during 12 and 20 kHz stimulation. This shows a reduction in midbrain responses 7 days following acute noise exposure with partial recovery seen by 14 days. *t*-values are color coded.

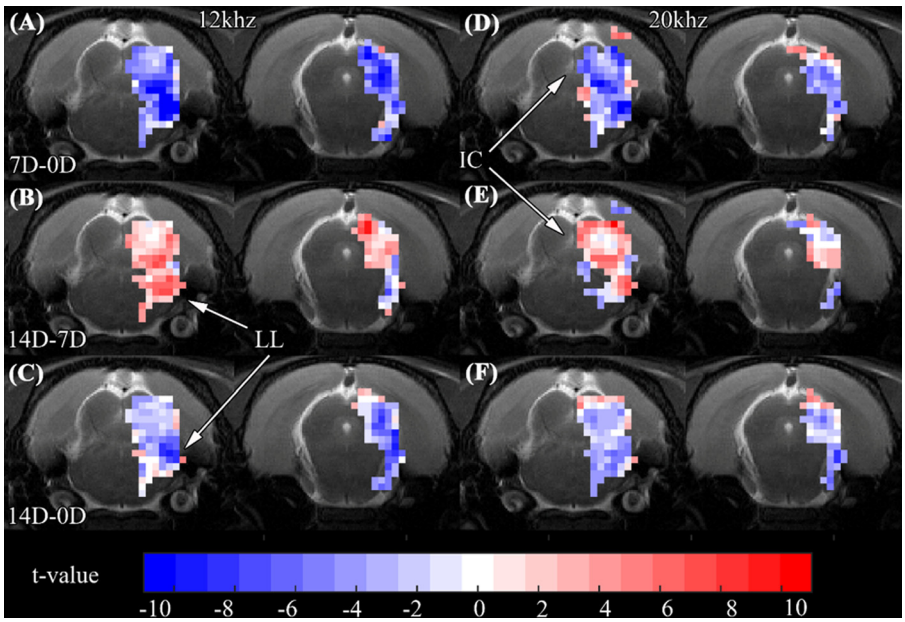

FIG. 6. (Color online) Group averaged *t*-value difference maps during 12 and 20 kHz stimulation overlaid on an anatomical image. The *t*-value differences were computed by subtracting group averaged activation maps. (A) 7D–0D, 12 kHz; (B) 14D–7D, 12 kHz; (C) 14D–0D, 12 kHz; (D) 7D–0D, 20 kHz; (E) 14D–7D, 20 kHz; (F) 14D–0D, 20 kHz. Primarily positive *t*-value differences (red voxels) are observed in 14D–7D during both frequencies. Primarily negative *t*-value differences (blue voxels) are observed in 7D–0D and 14D–0D. This shows a reduction in midbrain responses following acute noise exposure with timescale of a week. The color bar indicates the *t*-value difference.

2004), both spontaneous and task-evoked. The BOLD signal amplitude due to a task, such as sound stimulation, is further related to the amplitude of the baseline spontaneous activity. Hyder, Smith, and colleagues measured BOLD and extracellular neural activity from the somatosensory cortex of rats (Hyder *et al.*, 2002; Smith *et al.*, 2002). They observed that the task-evoked BOLD signal was smaller when the amplitude of spontaneous activity was larger, and vice versa.

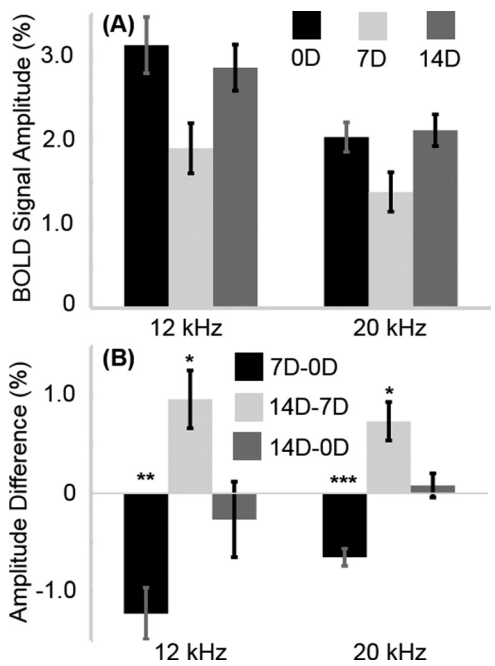

FIG. 7. (A) BOLD signal amplitudes (%) in the IC (mean and standard error) at 0D, 7D, and 14D obtained from the ROIs in Fig. 2. In general, signals are highest at 0D, lowest at 7D, and return to near pre-exposure levels at 14D. (B) Differences in signal amplitude (%) in the IC at 0D, 7D, and 14D. There is a statistically significant reduction in fMRI responses from the auditory midbrain 7 days following acute noise exposure and partial recovery by 14 days after. "*," "**," and "***" indicate $p < 0.05$, $p < 0.01$, and $p < 0.001$, respectively (computed by ANOVA followed by Tukey's HSD test).

Relating to the results of this study, the BOLD signal amplitudes in the LL and IC 7 days after acute noise exposure are reduced but partially recover by 14 days after. These fMRI changes at seven days are likely related to the increased midbrain spontaneous activity reported in the above studies (Ma *et al.*, 2006; Mulders and Robertson,

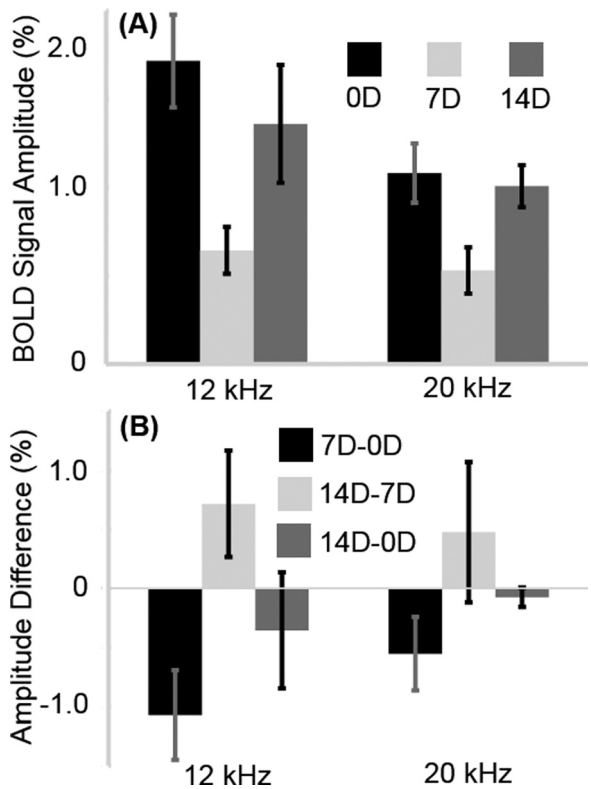

FIG. 8. (A) BOLD signal amplitudes (%) in the LL (mean and standard error) at 0D, 7D, and 14D obtained from the ROIs in Fig. 2. In general, signals are highest at 0D, lowest at 7D, and return to near pre-exposure levels at 14D. (B) Differences in signal amplitude (%) in the LL at 0D, 7D, and 14D. There is a reduction in fMRI responses from the auditory midbrain 7 days following acute noise exposure and partial recovery by 14 days after. The trends are similar to those in the IC.

2009; Dong *et al.*, 2010; Mulders *et al.*, 2010; Mulders and Robertson, 2011; Manzoor *et al.*, 2012; Robertson *et al.*, 2013; Coomber *et al.*, 2014; Basura *et al.*, 2015; Hesse *et al.*, 2016; Wu *et al.*, 2016). By 14 days, the increased activity likely receded as the relatively mild noise exposure induced only a short duration temporary threshold shift (see Fig. 3). These changes in spontaneous activity occur without significant hearing threshold shift at the time of measurement and across multiple auditory nuclei of the midbrain.

B. Central gain

Central gain is another mechanism that may contribute to the BOLD signal changes following acute acoustic noise exposure. Acute exposure leads to degeneration of auditory nerve synapses within 24 h of exposure and these nerves stop responding to sound (Kujawa and Liberman, 2009). However, subjects are still able to detect sounds. This likely reflects increased gain in the central auditory system following exposure (Auerbach *et al.*, 2014; Chambers *et al.*, 2016). Early evidence for increased central gain came from electrical stimulation of the cochlear nucleus and IC coupled with behavioral measurements of the stimulation threshold (Gerken *et al.*, 1984). The response threshold following 110 dB SPL, 48 h exposure was surprisingly decreased relative to that before exposure. More direct evidence for increased central gain came from evoked response studies (Popelar *et al.*, 1987; Salvi *et al.*, 1990; Syka *et al.*, 1994). A broadband 120 dB SPL, 1 h exposure temporarily shifted response thresholds in the auditory nerve, IC, and auditory cortex (AC). In the AC, the response amplitude to high intensity sound stimulation was larger than before exposure and persisted at least 24 h post exposure (Popelar *et al.*, 1987). A 2 kHz, 105 dB SPL exposure induced a permanent threshold shift from 2 to 8 kHz (Salvi *et al.*, 1990). In the IC, the response amplitude during 0.5 kHz stimulation was enhanced.

In this study, suprathreshold ABR wave IV amplitude is increased at 7D compared with 0D (see Fig. 4). This may reflect increases in central gain in the midbrain. However, BOLD signals are affected by both spontaneous activity and central gain. Therefore, spontaneous activity changes may partially mask central gain changes in fMRI. Also note that the hours and days long timescales of the early studies in the above paragraph were considerably shorter than the weeks long timescale in this study. Recently, near complete lesioning of synapses in mice was found to eliminate the ABR and acoustic startle reflex, but subjects were still able to perceive tones (Chambers *et al.*, 2016). Lesioning progressively reduced sound evoked auditory nerve responses over the course of weeks. In the midbrain, however, multi-unit activity was greatly reduced 7 days post-lesioning but partial recovery was observed at 30 days. In the AC, the activity at 30 days was even above those of control subjects. Increased central gain with weeks long timescale may be partly responsible for the recovery of midbrain responses observed in this study.

C. Synaptopathy

A recently discovered danger of acute acoustic exposures that cause temporary threshold shifts is rapid loss, within 24 h, of synapses (synaptopathy) at the junction of inner hair cells and auditory nerve fibers (Plack *et al.*, 2014; Kujawa and Liberman, 2015). This synaptopathy occurs without hair cell loss and the spiral ganglion cells of the auditory nerve degenerate only long afterward. Further, the lost synapses concentrate in fibers with high thresholds and low spontaneous discharge rates (Furman *et al.*, 2013). This condition has been named hidden hearing loss (Plack *et al.*, 2014). Hidden hearing loss may cause subjects with a history of noise exposure to have speech discrimination difficulties, especially in noise, and sound temporal processing difficulties. Further, hidden hearing loss may also be associated with tinnitus. The synaptopathy was originally observed to be permanent, but different species or exposure levels may allow partial recovery (Liu *et al.*, 2012; Shi *et al.*, 2016). However, the recovered synapses still suffer from functional deficits.

In this study, decreased suprathreshold ABR wave I amplitude at 14D (see Fig. 4), relative to 0D, agrees with rodent studies of acute noise induced synaptopathy (Kujawa and Liberman, 2009; Lin *et al.*, 2011; Furman *et al.*, 2013; Hickox and Liberman, 2014). Further, the small increase of wave IV at 7D, and small decrease at 14D, agrees with earlier rodent studies which observed that wave IV is similar, and sometimes increased, after noise (Ruttiger *et al.*, 2013; Mohrle *et al.*, 2016). Since the acoustic stimulus during fMRI was at a high 80–90 dB SPL, the loss of high threshold auditory nerve fibers would be expected to reduce the input to the midbrain and reduce BOLD signals, as observed at 7D and 14D. However, this mechanism likely occurs alongside changes in midbrain spontaneous activity and central gain.

The increased suprathreshold wave I amplitude at 7D (see Fig. 4) may be related to forward masking of the click sound by the preceding click sound (100 ms earlier). Loss of low spontaneous rate fibers in synaptopathy has recently been postulated to increase wave I amplitude in a forward masking situation (see Fig. 1 of Mehraei *et al.*, 2017) because such fibers slow down recovery of the wave after the masker (Mehraei *et al.*, 2017). Note that 7D is before the majority of wave I measurement time points reported (Kujawa and Liberman, 2009; Lin *et al.*, 2011; Furman *et al.*, 2013; Hickox and Liberman, 2014), which typically range from 1 to 8 weeks post exposure. Also, the exposure in this study is of relatively short duration (15 min) compared with exposures in earlier synaptopathy studies.

D. Technical considerations

fMRI generates acoustic noise which may affect hearing and processing of the acoustic stimulus. In this study, there are two sources of acoustic exposure during fMRI, scanner acoustic noise and the acoustic stimuli. The SPL of the stimuli are 90 (12 kHz) and 80 (20 kHz) dB. Each subject hears each stimulus for a total of 10 min after the three time points. The SPL of the scanner noise is difficult to measure as such a measurement would have to be done in the ear canal and

inside the scanner. Considering that robust fMRI responses are observed, the scanner SPL likely does not exceed 80 dB. Each subject hears the scanner for 140 min. In comparison, the study's acute acoustic exposure is 100 dB SPL for 15 min. Converting from dB to acoustic energy, the acute exposure delivered 15.0 times more energy than the 12 kHz stimulus, 150.0 times more energy than the 20 kHz stimulus, and 10.7 times more energy than the scanner. Therefore, fMRI acoustic noise is small compared with the acute exposure.

Also, the setup in this study has been used to study the rat central auditory system and obtained results that agreed with previous understanding and added new insight. For example, fMRI responses to acoustic stimulation has been observed in the cochlear nucleus, superior olivary complex, LL, IC, medial geniculate body, and AC (Cheung *et al.*, 2012a). Tonal stimuli enabled mapping the dorsal to ventral arrangement of tonotopic organization in the IC (Cheung *et al.*, 2012b). Varying the SPL of the stimulus enabled observing different SPL dependences across the auditory system (Zhang *et al.*, 2013). Binaural stimulation with different SPLs in the two ears enabled studying interaural level difference processing across multiple auditory nuclei (Lau *et al.*, 2013). More recently, we have begun investigating the impact of long-term, moderate SPL noise exposure (no hearing loss) across the auditory system (Lau *et al.*, 2015a; Lau *et al.*, 2015b). Therefore, fMRI can complement existing methods, such as electrophysiology, and help advance the understanding of important problems such as noise exposure.

The subjects used in fMRI ($N = 10$) and ABR ($N = 4$) in this study were separate. Also, ABRs were recorded with 0.1 ms click sounds in this study. Recording with clicks instead of pure tones does not permit the hearing threshold to be measured at specific frequencies. However, the clicks stimulate much of the rat audible frequency range. This enables detecting the presence (or absence) of significant threshold shifts, which is the primary purpose for recording ABRs in this study.

Hearing threshold elevations can reduce fMRI responses in the central auditory system. In this study, the BOLD signal in the IC at 7D during 12 kHz stimulation was 39% smaller than that at 0D. BOLD signals in the IC have been observed to increase almost linearly with acoustic stimulus SPL (see Fig. 5 of Zhang *et al.*, 2013). Assuming that threshold elevation is equivalent to stimulus SPL reduction, and assuming that the 39% BOLD difference were due solely to threshold elevation, the required elevation would be ~30 dB (Zhang *et al.*, 2013). Such a large elevation is not observed in the ABRs between 0D and 7D or 14D. Therefore, the signal reduction is primarily due to central auditory changes.

This study employed female rats as subjects, and males and females differ in their susceptibility to high intensity noise (Ward, 1966; McFadden *et al.*, 1999). Males experience more hearing loss at low frequencies while females experience more loss at high frequencies. These differences may be closely related to the sex hormones, such as estrogen, as hearing declines rapidly during menopause (Svedbrant *et al.*, 2015) and noise induced threshold shifts fluctuate with the menstrual cycle (Davis and Ahroon, 1982). The estrogen receptor β has been demonstrated to protect against noise induced threshold shifts (Meltser *et al.*, 2008). Considering the gender differences, future studies can examine central auditory changes following acute noise exposures in males and females.

V. CONCLUSION

fMRI was performed on rat subjects that received noise exposure of high SPL and short duration. The acute acoustic exposure reduced fMRI signals from the auditory midbrain at 7 days after exposure, compared with pre-exposure levels. By 14 days after, partial recovery of signals is seen. At these time points, near-threshold ABRs did not differ significantly from pre-exposure levels. Therefore, acute exposure leads to functional changes in the auditory midbrain with timescale of weeks.

ACKNOWLEDGMENTS

This research was supported by the Hong Kong Health and Medical Research Fund (Grant No. 11122581), General Research Fund (Grant No. 21201217), and start-up funding from the City University of Hong Kong. The authors would also like to acknowledge Simon Chan of the School of Biomedical Sciences, The University of Hong Kong, for providing technical support to this project. B.Y. and E.W. contributed equally to this work.

[1]See supplementary material at https://doi.org/10.1121/1.5030920 for the BOLD signals from the lateral lemniscus and inferior colliculus at each time point and stimulation frequency.

Abdoli, S., Ho, L. C., Zhang, J. W., Dong, C. M., Lau, C., and Wu, E. X. (**2016**). "Diffusion tensor imaging reveals changes in the adult rat brain following long-term and passive moderate acoustic exposure," J. Acoust. Soc. Am. **140**, 4540.

Auerbach, B. D., Rodrigues, P. V., and Salvi, R. J. (**2014**). "Central gain control in tinnitus and hyperacusis," Front. Neurol. **5**, 206.

Bach, J. P., Lüpke, M., Dziallas, P., Wefstaedt, P., Uppenkamp, S., Seifert, H., and Nolte, I. (**2013**). "Functional magnetic resonance imaging of the ascending stages of the auditory system in dogs," BMC Vet Res. **9**, 210.

Basura, G. J., Koehler, S. D., and Shore, S. E. (**2015**). "Bimodal stimulus timing-dependent plasticity in primary auditory cortex is altered after noise exposure with and without tinnitus," J. Neurophysiol. **114**, 3064–3075.

Baumann, S., Griffiths, T. D., Sun, L., Petkov, C. I., Thiele, A., and Rees, A. (**2011**). "Orthogonal representation of sound dimensions in the primate midbrain," Nat. Neurosci. **14**, 423–425.

Bilecen, D., Seifritz, E., Radu, E. W., Schmid, N., Wetzel, S., Probst, R., and Scheffler, K. (**2000**). "Cortical reorganization after acute unilateral hearing loss traced by fMRI," Neurology **54**, 765–767.

Boumans, T., Theunissen, F. E., Poirier, C., and Van Der Linden, A. (**2007**). "Neural representation of spectral and temporal features of song in the auditory forebrain of zebra finches as revealed by functional MRI," Eur. J. Neurosci. **26**, 2613–2626.

Brown, T. A., Joanisse, M. F., Gati, J. S., Hughes, S. M., Nixon, P. L., Menon, R. S., and Lomber, S. G. (**2013**). "Characterization of the blood-oxygen level-dependent (BOLD) response in cat auditory cortex using high-field fMRI," Neuroimage **64**, 458–465.

Butler, B. E., Hall, A. J., and Lomber, S. G. (**2015**). "High-field functional imaging of pitch processing in auditory cortex of the cat," PLoS One **10**, e0134362.

Chambers, A. R., Resnik, J., Yuan, Y., Whitton, J. P., Edge, A. S., Liberman, M. C., and Polley, D. B. (**2016**). "Central gain restores auditory processing following near-complete cochlear denervation," Neuron **89**, 867–879.

Cheung, M. M., Lau, C., Zhou, I. Y., Chan, K. C., Cheng, J. S., Zhang, J. W., Ho, L. C., and Wu, E. X. (**2012a**). "BOLD fMRI investigation of the rat auditory pathway and tonotopic organization," Neuroimage **60**, 1205–1211.

Cheung, M. M., Lau, C., Zhou, I. Y., Chan, K. C., Zhang, J. W., Fan, S. J., and Wu, E. X. (**2012b**). "High fidelity tonotopic mapping using swept source functional magnetic resonance imaging," Neuroimage **61**, 978–986.
Coomber, B., Berger, J. I., Kowalkowski, V. L., Shackleton, T. M., Palmer, A. R., and Wallace, M. N. (**2014**). "Neural changes accompanying tinnitus following unilateral acoustic trauma in the guinea pig," Eur. J. Neurosci. **40**, 2427–2441.
Davis, M. J., and Ahroon, W. A. (**1982**). "Fluctuations in susceptibility to noise-induced temporary threshold shift as influenced by the menstrual cycle," J. Aud. Res. **22**, 173–187.
Dong, S., Mulders, W. H., Rodger, J., Woo, S., and Robertson, D. (**2010**). "Acoustic trauma evokes hyperactivity and changes in gene expression in guinea-pig auditory brainstem," Eur. J. Neurosci. **31**, 1616–1628.
Friederici, A. D., Meyer, M., and von Cramon, D. Y. (**2000**). "Auditory language comprehension: An event-related fMRI study on the processing of syntactic and lexical information," Brain Lang. **75**, 289–300.
Furman, A. C., Kujawa, S. G., and Liberman, M. C. (**2013**). "Noise-induced cochlear neuropathy is selective for fibers with low spontaneous rates," J. Neurophysiol. **110**, 577–586.
Gao, P. P., Zhang, J. W., Chan, R. W., Leong, A. T., and Wu, E. X. (**2015a**). "BOLD fMRI study of ultrahigh frequency encoding in the inferior colliculus," Neuroimage **114**, 427–437.
Gao, P. P., Zhang, J. W., Cheng, J. S., Zhou, I. Y., and Wu, E. X. (**2014**). "The inferior colliculus is involved in deviant sound detection as revealed by BOLD fMRI," Neuroimage **91**, 220–227.
Gao, P. P., Zhang, J. W., Fan, S. J., Sanes, D. H., and Wu, E. X. (**2015b**). "Auditory midbrain processing is differentially modulated by auditory and visual cortices: An auditory fMRI study," Neuroimage **123**, 22–32.
Gerken, G. M., Saunders, S. S., and Paul, R. E. (**1984**). "Hypersensitivity to electrical stimulation of auditory nuclei follows hearing loss in cats," Hear. Res. **13**, 249–259.
Gu, J. W., Halpin, C. F., Nam, E. C., Levine, R. A., and Melcher, J. R. (**2010**). "Tinnitus, diminished sound-level tolerance, and elevated auditory activity in humans with clinically normal hearing sensitivity," J. Neurophysiol. **104**, 3361–3370.
Hall, A. J., Butler, B. E., and Lomber, S. G. (**2016**). "The cat's meow: A high-field fMRI assessment of cortical activity in response to vocalizations and complex auditory stimuli," Neuroimage **127**, 44–57.
Hesse, L. L., Bakay, W., Ong, H. C., Anderson, L., Ashmore, J., McAlpine, D., Linden, J., and Schaette, R. (**2016**). "Non-monotonic relation between noise exposure severity and neuronal hyperactivity in the auditory midbrain," Front. Neurol. **7**, 1–13.
Hickox, A. E., and Liberman, M. C. (**2014**). "Is noise-induced cochlear neuropathy key to the generation of hyperacusis or tinnitus?," J. Neurophysiol. **111**, 552–564.
Holland, S. K., Karunanayaka, P., Rajagopal, A., and Smith, K. (**2008**). "fMRI evidence for central auditory processing of speech in deaf infants under sedation," J. Acoust. Soc. Am. **123**, 3319.
Hyder, F., Rothman, D. L., and Shulman, R. G. (**2002**). "Total neuroenergetics support localized brain activity: Implications for the interpretation of fMRI," Proc. Natl. Acad. Sci. U.S.A. **99**, 10771–10776.
Jancke, L., Gaab, N., Wustenberg, T., Scheich, H., and Heinze, H. J. (**2001**). "Short-term functional plasticity in the human auditory cortex: An fMRI study," Brain Res. Cogn. Brain Res. **12**, 479–485.
Kayser, C., Petkov, C. I., Augath, M., and Logothetis, N. K. (**2007**). "Functional imaging reveals visual modulation of specific fields in auditory cortex," J. Neurosci. **27**, 1824–1835.
Koelsch, S., Fritz, T., Schulze, K., Alsop, D., and Schlaug, G. (**2005**). "Adults and children processing music: An fMRI study," Neuroimage **25**, 1068–1076.
Kujawa, S. G., and Liberman, M. C. (**2009**). "Adding insult to injury: Cochlear nerve degeneration after 'temporary' noise-induced hearing loss," J. Neurosci. **29**, 14077–14085.
Kujawa, S. G., and Liberman, M. C. (**2015**). "Synaptopathy in the noise-exposed and aging cochlea: Primary neural degeneration in acquired sensorineural hearing loss," Hear. Res. **330**, 191–199.
Lanting, C. P., De Kleine, E., Bartels, H., and Van Dijk, P. (**2008**). "Functional imaging of unilateral tinnitus using fMRI," Acta. Otolaryngol. **128**, 415–421.
Lau, C., Pienkowski, M., Zhang, J. W., McPherson, B., and Wu, E. X. (**2015a**). "Chronic exposure to broadband noise at moderate sound pressure levels spatially shifts tone-evoked responses in the rat auditory midbrain," Neuroimage **122**, 44–51.
Lau, C., Zhang, J. W., Cheng, J. S., Zhou, I. Y., Cheung, M. M., and Wu, E. X. (**2013**). "Noninvasive fMRI investigation of interaural level difference processing in the rat auditory subcortex," PLoS One **8**, e70706.
Lau, C., Zhang, J. W., McPherson, B., Pienkowski, M., and Wu, E. X. (**2015b**). "Long-term, passive exposure to non-traumatic acoustic noise induces neural adaptation in the adult rat medial geniculate body and auditory cortex," Neuroimage **107**, 1–9.
Liberman, M. C. (**2015**). "Hidden hearing loss," Sci. Am. **313**, 48–53.
Lin, H. W., Furman, A. C., Kujawa, S. G., and Liberman, M. C. (**2011**). "Primary neural degeneration in the guinea pig cochlea after reversible noise-induced threshold shift," J. Assoc. Res. Otolaryngol. **12**, 605–616.
Liu, L., Wang, H., Shi, L., Almuklass, A., He, T., Aiken, S., Bance, M., Yin, S., and Wang, J. (**2012**). "Silent damage of noise on cochlear afferent innervation in guinea pigs and the impact on temporal processing," PLoS One **7**, e49550.
Logothetis, N. K., Pauls, J., Augath, M., Trinath, T., and Oeltermann, A. (**2001**). "Neurophysiological investigation of the basis of the fMRI signal," Nature **412**, 150–157.
Logothetis, N. K., and Wandell, B. A. (**2004**). "Interpreting the BOLD signal," Annu. Rev. Physiol. **66**, 735–769.
Ma, W. L., Hidaka, H., and May, B. J. (**2006**). "Spontaneous activity in the inferior colliculus of CBA/J mice after manipulations that induce tinnitus," Hear. Res. **212**, 9–21.
Maeder, P. P., Meuli, R. A., Adriani, M., Bellmann, A., Fornari, E., Thiran, J. P., Pittet, A., and Clarke, S. (**2001**). "Distinct pathways involved in sound recognition and localization: A human fMRI study," Neuroimage **14**, 802–816.
Manzoor, N. F., Licari, F. G., Klapchar, M., Elkin, R. L., Gao, Y., Chen, G., and Kaltenbach, J. A. (**2012**). "Noise-induced hyperactivity in the inferior colliculus: Its relationship with hyperactivity in the dorsal cochlear nucleus," J. Neurophysiol. **108**, 976–988.
McFadden, S. L., Henselman, L. W., and Zheng, X. Y. (**1999**). "Sex differences in auditory sensitivity of chinchillas before and after exposure to impulse noise," Ear Hear. **20**, 164–174.
Mehraei, G., Gallardo, A. P., Shinn-Cunningham, B. G., and Dau, T. (**2017**). "Auditory brainstem response latency in forward masking, a marker of sensory deficits in listeners with normal hearing thresholds," Hear. Res. **346**, 34–44.
Meltser, I., Tahera, Y., Simpson, E., Hultcrantz, M., Charitidi, K., Gustafsson, J. A., and Canlon, B. (**2008**). "Estrogen receptor beta protects against acoustic trauma in mice," J. Clin. Invest. **118**, 1563–1570.
Mohrle, D., Ni, K., Varakina, K., Bing, D., Lee, S. C., Zimmermann, U., Knipper, M., and Ruttiger, L. (**2016**). "Loss of auditory sensitivity from inner hair cell synaptopathy can be centrally compensated in the young but not old brain," Neurobiol. Aging **44**, 173–184.
Mulders, W. H., and Robertson, D. (**2009**). "Hyperactivity in the auditory midbrain after acoustic trauma: Dependence on cochlear activity," Neuroscience **164**, 733–746.
Mulders, W. H., and Robertson, D. (**2011**). "Progressive centralization of midbrain hyperactivity after acoustic trauma," Neuroscience **192**, 753–760.
Mulders, W. H., Seluakumaran, K., and Robertson, D. (**2010**). "Efferent pathways modulate hyperactivity in inferior colliculus," J. Neurosci. **30**, 9578–9587.
National Institute on Deafness and Other Communication Disorders (NIDCD) (**2014**). Noise-Induced Hearing Loss (Bethesda, MD).
National Institute for Occupational Safety and Health (NIOSH) (**1998**). *Criteria for a Recommended Standard—Occupational Noise Exposure* (Washington, DC).
Ogawa, S., Lee, T. M., Kay, A. R., and Tank, D. W. (**1990**). "Brain magnetic-resonance-imaging with contrast dependent on blood oxygenation," Proc. Natl. Acad. Sci. U.S.A. **87**, 9868–9872.
Ortiz-Rios, M., Azevedo, F. A. C., Kusmierek, P., Balla, D. Z., Munk, M. H., Keliris, G. A., Logothetis, N. K., and Rauschecker, J. P. (**2017**). "Widespread and opponent fMRI signals represent sound location in macaque auditory cortex," Neuron **93**, 971–983.
Paxinos, G., and Watson, C. (**2005**). *The Rat Brain in Stereotaxic Coordinates* (Elsevier Academic, Cambridge, MA).
Plack, C. J., Barker, D., and Prendergast, G. (**2014**). "Perceptual consequences of 'hidden' hearing loss," Trends Hear. **18**, 1–11.
Popelar, J., Syka, J., and Berndt, H. (**1987**). "Effect of noise on auditory evoked responses in awake guinea pigs," Hear. Res. **26**, 239–247.
Robertson, D., Bester, C., Vogler, D., and Mulders, W. H. (**2013**). "Spontaneous hyperactivity in the auditory midbrain: Relationship to afferent input," Hear. Res. **295**, 124–129.

Ruttiger, L., Singer, W., Panford-Walsh, R., Matsumoto, M., Lee, S. C., Zuccotti, A., Zimmermann, U., Jaumann, M., Rohbock, K., Xiong, H., and Knipper, M. (**2013**). "The reduced cochlear output and the failure to adapt the central auditory response causes tinnitus in noise exposed rats," PLoS One **8**, e57247.

Salvi, R. J., Saunders, S. S., Gratton, M. A., Arehole, S., and Powers, N. (**1990**). "Enhanced evoked response amplitudes in the inferior colliculus of the chinchilla following acoustic trauma," Hear. Res. **50**, 245–257.

Schmithorst, V. J., Holland, S. K., Ret, J., Duggins, A., Arjmand, E., and Greinwald, J. (**2005**). "Cortical reorganization in children with unilateral sensorineural hearing loss," Neuroreport **16**, 463–467.

Shi, L., Chang, Y., Li, X., Aiken, S. J., Liu, L., and Wang, J. (**2016**). "Coding deficits in noise-induced hidden hearing loss may stem from incomplete repair of ribbon synapses in the cochlea," Front. Neurosci. **10**, 231.

Smith, A. J., Blumenfeld, H., Behar, K. L., Rothman, D. L., Shulman, R. G., and Hyder, F. (**2002**). "Cerebral energetics and spiking frequency: The neurophysiological basis of fMRI," Proc. Natl. Acad. Sci. U.S.A. **99**, 10765–10770.

Smits, M., Kovacs, S., de Ridder, D., Peeters, R. R., van Hecke, P., and Sunaert, S. (**2007**). "Lateralization of functional magnetic resonance imaging (fMRI) activation in the auditory pathway of patients with lateralized tinnitus," Neuroradiology **49**, 669–679.

Svedbrant, J., Bark, R., Hultcrantz, M., and Hederstierna, C. (**2015**). "Hearing decline in menopausal women—A 10-year follow-up," Acta Otolaryngol. **135**, 807–813.

Syka, J., Rybalko, N., and Popelar, J. (**1994**). "Enhancement of the auditory cortex evoked responses in awake guinea pigs after noise exposure," Hear. Res. **78**, 158–168.

Tanji, K., Leopold, D. A., Ye, F. Q., Zhu, C., Malloy, M., Saunders, R. C., and Mishkin, M. (**2010**). "Effect of sound intensity on tonotopic fMRI maps in the unanesthetized monkey," Neuroimage **49**, 150–157.

Van Meir, V., Boumans, T., De Groof, G., Van Audekerke, J., Smolders, A., Scheunders, P., Sijbers, J., Verhoye, M., Balthazart, J., and Van der Linden, A. (**2005**). "Spatiotemporal properties of the BOLD response in the songbirds' auditory circuit during a variety of listening tasks," Neuroimage **25**, 1242–1255.

Voss, H. U., Tabelow, K., Polzehl, J., Tchernichovski, O., Maul, K. K., Salgado-Commissariat, D., Ballon, D., and Helekar, S. A. (**2007**). "Functional MRI of the zebra finch brain during song stimulation suggests a lateralized response topography," Proc. Natl. Acad. Sci. U.S.A. **104**, 10667–10672.

Ward, W. D. (**1966**). "Temporary threshold shift in males and females," J. Acoust. Soc. Am. **40**, 478–485.

Wong, E., Yang, B., Du, L., Ho, W. H., Lau, C., Ke, Y., Chan, Y. S., Yung, W. H., and Wu, E. X. (**2017**). "The multi-level impact of chronic intermittent hypoxia on central auditory processing," Neuroimage **156**, 232–239.

Wu, C. M., and Lin, Y. S. (**2008**). "Neural correlates on Chinese speech production: An fMRI study," J. Acoust. Soc. Am. **125**, 3075.

Wu, C., Martel, D. T., and Shore, S. E. (**2016**). "Increased synchrony and bursting of dorsal cochlear nucleus fusiform cells correlate with tinnitus," J. Neurosci. **36**, 2068–2073.

Zhang, J. W., Lau, C., Cheng, J. S., Xing, K. K., Zhou, I. Y., Cheung, M. M., and Wu, E. X. (**2013**). "Functional magnetic resonance imaging of sound pressure level encoding in the rat central auditory system," Neuroimage **65**, 119–126.